



# SHUNT ACTIVE FILTERS WITH MODEL PREDICTIVE AND FUZZY CONTROL FIXED SWITCHING FREQUENCY

O.SAIDULU REDDY

Assistant Professor

Malla Reddy College Of Engineering and Technology, India

**ABSTRACT :** In this project we are implementing the Model Predictive Control (MPC) algorithm with fuzzy logic controller and for active power filter application. Therefore the proposed control consist of many merits of finite control set MPC which will enhance the generation of harmonics spectrum waveform .according to the modulation algorithm which is depend upon the cost function ration with different output vector which included the MPC .here we are included the fuzzy logic controller which works like a human brain for the better performance and also reduce the harmonics distortion and reactive power compensation .therefore the cost function-based modulator is developed In order to decreases the current ripple which have been estimated. Therefore according to this we can provide an effective and straightforward single loop controller, maintaining an excellent dynamic performance with the modulated output and it is self synchronizing with the grid. Therefore according to the promising method which is applied to control of a shunt active filter for harmonic content reduction in order to compensation of reactive power by using simulation we can observe the MPC is a viable control solution for active filtering systems.

**Index Terms—**Active filters, harmonic distortion, model predictive control (MPC), power filters, power quality, smart grids and fuzzy control.

## Introduction

Power quality level in modern electrical grids is a vital issue to ensure reliability, security, and efficiency [1]. This is currently becoming extremely important due to the proliferation of nonlinear loads, power conversion systems, renewable energy sources, distributed generation sources, and plug-in electric vehicles [2]. These studies resulted in a broad family of devices, such as active and hybrid power filters [5], static compensators [6], [7], static VAR compensators [8], unified power flow/quality controllers, and dynamic voltage restorers.

In particular, active power filters allow us to increase the overall system power quality and they are not affected by the limits of their passive counterparts, such as the introduction of resonances onto the power system, impossibility of current limiting (other than fuses), and overloaded operation if the supply voltage quality deteriorates [9].

However, the control of an active filter [10] requires fast dynamic performances and represents a challenging control problem, which may not be able to be addressed by applying linear control techniques. In fact, as a high control bandwidth is required, it may happen that the required sampling frequency becomes excessively high. Moreover, supply disturbances may be hard to suppress using classical PI controllers [11], [12].

Techniques that reduce the number of measurements required by the system have also been investigated, typically based on time-domain controllers and an appropriate observer. Finally, dead-beat control strategies have also been considered, coupled with a PI-based dc-Link voltage control. Model predictive control (MPC) has been recently adopted for power electronics converters control, due to the several benefits it can provide, such as fast tracking response and simple inclusion of system nonlinearities and constraints in the controller. Christo Ananth et al.[4] presented a brief outline on Electronic Devices and Circuits which forms the basis of the Clampers and Diodes.MPC considers the system model for predicting its future behavior and determining the best control action on the basis of a cost function minimization procedure. Finite control set MPC (FCS–MPC) is a model-based control strategy applicable to systems with a finite number of possible control actions, such as power electronic converters.

This technique has been successfully applied for the control of three-phase inverters matrix converters, power control in an active front end rectifiers and regulation of both electrical and mechanical variables in drive system applications. The lack of a modulator, although being an advantage for the transient performance of the system, it is also a drawback under steady-state conditions when the high bandwidth of the control is not necessary and the higher current ripple, due to the limited set of available control actions, is more evident. This paper presents a novel Finite Control Set Modulated MPC (FCS–M2 PC) algorithm suitable for SAF control, which retains most of the advantages of the MPC,

such as the presence of a cost function and the use of a single loop for improved responsivity and larger bandwidth, but exploits a modulator for reducing the current ripple.

### SYSTEM DESCRIPTION AND MODELING

A SAF is realized by connecting a voltage source converter (VSC) to the ac grid through filter inductors in a rectifier configuration. The dc side is connected to a capacitor as depicted in Fig. 1, and thus, it is able to manage only reactive power. In such configuration, the SAF is able to produce any set of balanced currents and, therefore, compensates the reactive power and current harmonics drawn by a nonlinear load; clearly the SAF filtering capabilities are limited by the VSC-rated power and control bandwidth.

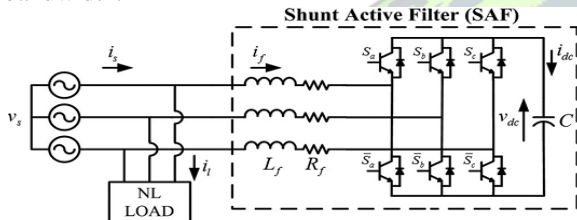


Fig. 1. Adopted structure of three-wires SAF

When a balanced system is considered, it is possible to reduce the system order to the third order, represented in the abc-frame by the state variables  $i_{fa}(t)$ ,  $i_{fb}(t)$ , and  $V_{dc}(t)$ . Neglecting the nonlinearities introduced by the inverter and the equivalent impedance of the grid, the SAF currents equations can be expressed as follows:

$$\begin{cases} \frac{di_{fa}(t)}{dt} = \frac{1}{L_f} v_{sa}(t) - \frac{R_f}{L_f} i_{fa}(t) - \frac{1}{3L_f} [2s_a(t) - s_b(t) - s_c(t)] \\ \frac{di_{fb}(t)}{dt} = \frac{1}{L_f} v_{sb}(t) - \frac{R_f}{L_f} i_{fb}(t) - \frac{1}{3L_f} [2s_b(t) - s_c(t) - s_a(t)] \\ \frac{dV_{dc}(t)}{dt} = \frac{1}{C} \{ [s_a(t) - s_c(t)] i_{fa}(t) + [s_b(t) - s_c(t)] i_{fb}(t) \} \end{cases} \quad (1)$$

where  $R_f$  and  $L_f$  are the filter inductor winding resistance and inductance.  $s_a(t)$ ,  $s_b(t)$ , and  $s_c(t)$  represent each leg state, equal to 1 or 0, respectively, when a positive or a negative voltage is produced at the leg output with respect to the dc-link neutral point. The dc-link voltage can be obtained by the converter switching functions and ac currents

$$\frac{dV_{dc}(t)}{dt} = \frac{1}{C} \{ [s_a(t) - s_c(t)] i_{fa}(t) + [s_b(t) - s_c(t)] i_{fb}(t) \} \quad (2)$$

Finally, the supply current can be obtained by the filter and load currents as

$$\begin{cases} i_{sa}(t) = i_{la}(t) + i_{fa}(t) \\ i_{sb}(t) = i_{lb}(t) + i_{fb}(t) \end{cases} \quad (3)$$

By combining (1)–(3), the SAF state space model can be derived and then discretized using the forward Euler method for control design purposes. The obtained system is shown as

$$\begin{cases} i_{fa}(k+1) = \left(1 - \frac{R_f h}{L_f}\right) i_{fa}(k) - \frac{h}{L_f} Q_1 \underline{s}(k) V_{dc}(k) + \frac{h}{L_f} v_{sa}(k) \\ i_{fb}(k+1) = \left(1 - \frac{R_f h}{L_f}\right) i_{fb}(k) - \frac{h}{L_f} Q_2 \underline{s}(k) V_{dc}(k) + \frac{h}{L_f} v_{sb}(k) \\ V_{dc}(k+1) = V_{dc}(k) + \frac{h}{C} P_1 \underline{s}(k) i_{fa}(k) \end{cases}$$

Where  $k$  represents the discrete sampling instant,  $h$  is the sampling time, and

$$Q_1 = \frac{1}{3} \begin{bmatrix} 2 & -1 & -1 \end{bmatrix} \quad Q_2 = \frac{1}{3} \begin{bmatrix} -1 & 2 & -1 \end{bmatrix} \quad (4)$$

$$P_1 = \begin{bmatrix} 1 & 0 & -1 \end{bmatrix} \quad P_2 = \begin{bmatrix} 0 & 1 & -1 \end{bmatrix}$$

$$\underline{s}(k) = [s_a(k) s_b(k) s_c(k)]^T$$

### SAF MODEL PREDICTIVE CONTROL

In FCS-MPC, due to the absence of a modulator, the only possible control actions are the ones generated by the eight possible inverter switching states

$$\underline{s}(k) \in \left\{ \begin{bmatrix} 0 \\ 0 \\ 0 \end{bmatrix}, \begin{bmatrix} 0 \\ 0 \\ 1 \end{bmatrix}, \begin{bmatrix} 0 \\ 1 \\ 0 \end{bmatrix}, \begin{bmatrix} 0 \\ 1 \\ 1 \end{bmatrix}, \begin{bmatrix} 1 \\ 0 \\ 0 \end{bmatrix}, \begin{bmatrix} 1 \\ 0 \\ 1 \end{bmatrix}, \begin{bmatrix} 1 \\ 1 \\ 0 \end{bmatrix}, \begin{bmatrix} 1 \\ 1 \\ 1 \end{bmatrix} \right\} \quad (5)$$

At the  $k$ th time instant the controller uses (4) to predict the future system state value for each possible control action in (6). A cost function is then computed using a combination of predicted system states and references. The optimal control is selected by choosing the inverter configuration associated to the minimum cost function value. This introduces a one-step delay in the system that must be compensated [21]. Combining the system model at the time instants  $k+1$  and  $k+2$ , and assuming that the supply voltages can be considered constant during a sampling period  $h$  of the control algorithm (i.e.,  $v_s(k) = v_s(k+1)$ ) the following system is obtained:

$$\underline{X}(K+2) = A_2 \left( \underline{s}(k+1) \right) \underline{X}(K) + B_2 \underline{U}(K) \quad (6)$$

The definition of the matrix elements are given in Appendix I, while  $\underline{X}(k)$  and  $\underline{U}(k)$ , shown in (8), represent the predicted values of active filter currents and voltages at the instant  $k+2$  and the supply voltages at the time instant  $k$ :

$$\begin{aligned} \underline{X}(K+2) &= [i_{fa}(k+2) i_{fb}(k+2) V_{dc}(k+2)]^T \\ \underline{U}(K) &= [v_{sa}(k) v_{sb}(k)]^T \end{aligned} \quad (7)$$

The load currents  $i_{la}$  and  $i_{lb}$  are assumed to be measurable in the considered configuration. Given

the high controller sampling frequency, it is acceptable to have

$$\begin{aligned} i_{sa}(k+2) &= i_{la}(k) + i_{fa}(k+2) \\ i_{sb}(k+2) &= i_{lb}(k) + i_{fb}(k+2) \end{aligned} \quad (8)$$

Hence the predicted system state is defined as

$$\underline{X}_p(k+2) = [i_{sa}(k+2) \ i_{sb}(k+2) \ V_{dc}(k+2)]^T \quad (9)$$

From (10) the control relevant variables the active power  $P_s$ , the reactive power  $Q_s$ , and the dc-Link voltage  $V_{dc}$  are predicted as shown

$$\begin{aligned} P_{sp}(k+2) &= \underline{v}_s^T(k) \begin{bmatrix} 2 & 1 & 0 \\ 1 & 2 & 0 \end{bmatrix} \underline{X}_p(k+2) \\ Q_{sp}(k+2) &= \underline{v}_s^T(k) \begin{bmatrix} 0 & \sqrt{3} & 0 \\ -\sqrt{3} & 0 & 0 \end{bmatrix} \underline{X}_p(k+2) \\ V_{dcp}(k+2) &= [0 \ 0 \ 1] \underline{X}_p(k+2) \end{aligned} \quad (9)$$

The 50-Hz grid voltages are supposed approximately constant in two consecutive sampling periods due to the much higher sampling frequency of the SAF control algorithm.

A block scheme of the complete active filter control for the case of FCS-MPC is shown in Fig. 2.

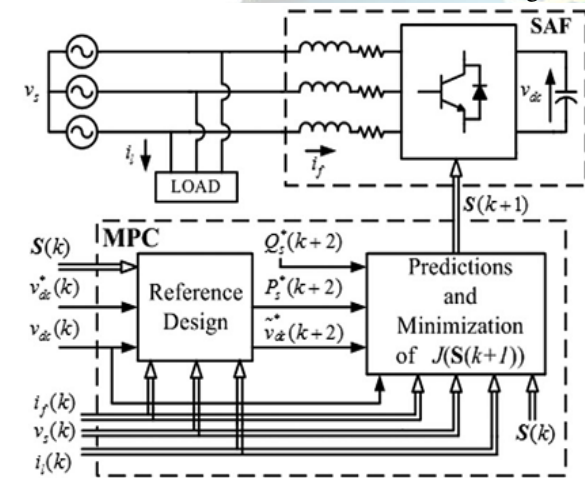


Fig. 2. Schematic diagram of a FCS-MPC.

### MODULATED MPC

One of the major strengths of the FCS-MPC is that it enables us to include in a single control law different control targets and system constraints. In this way, the traditional control of currents, voltages, or flux can be combined with other requirements, such as common mode voltage reduction, switching frequency minimization, and reactive power control.

To overcome this limit, but still maintain all the desired characteristics of FCS-MPC, this paper proposes the introduction of a suitable intrinsic modulation scheme. Consistently with the MPC approach, the cost function is used for selecting the converter states and application times that minimize

the equivalent cost in a sampling period. where  $J_i$  with  $i=0,1,2$  are the cost functions calculated as in (12) for the three vectors considered from the control, thus assuming  $S_i(k+1)$  equal, respectively, to the zero vector, the first active vector and the second active vector of the considered sector

$$J_{sect}(k+1) = d_0 J_0 + d_1 J_1 + d_2 J_2 \quad (10)$$

Similarly  $d_i$  are the duty cycles for the zero and active vectors. They are computed assuming that each duty cycle is proportional to the inverse of the corresponding cost function value, where  $K$  is a normalizing constant to be determined

$$\begin{cases} d_1 = K/J_1 \\ d_2 = K/J_2 \\ d_0 = K/J_0 \\ d_1 + d_2 + d_3 = 1 \end{cases} \quad (11)$$

Solving (11), the expression of the duty cycle is obtained as

$$\begin{aligned} d_1 &= \frac{J_2}{J_1 + J_2 + \frac{J_1 J_2}{J_0}} \\ d_2 &= \frac{J_1}{J_1 + J_2 + \frac{J_1 J_2}{J_0}} \end{aligned} \quad (12)$$

$$d_0 = 1 - (d_1 + d_2)$$

Essentially the cost function values  $J_i$  for each sector are calculated by using (7)–(12) and the corresponding application times are calculated from (15). The optimum sector is then determined by minimizing the cost function. The corresponding optimal duty cycles  $d(k+1) = [d_1(k+1) \ d_2(k+1) \ d_0(k+1)]^T$  are applied to the converter as represented in Fig. 3.

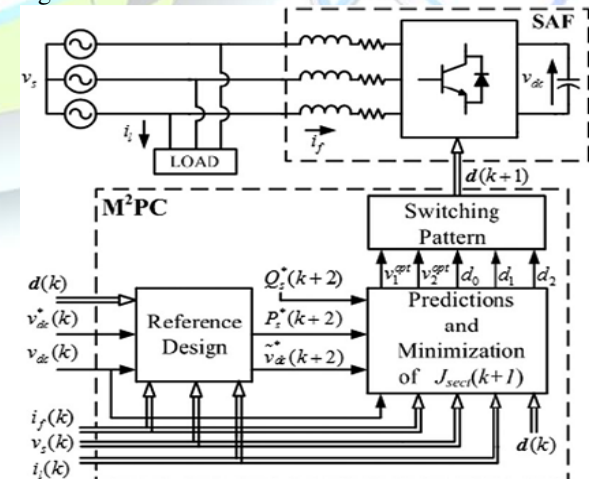


Fig. 3. Schematic diagram of the proposed FCS-M2PC



The switching sequence is generated from the two active and the three zero vector exactly as in a symmetrical SVM [37].

### REFERENCES PREDICTION

The coupling between active power  $P_s(k)$  and dc-Link voltage  $V_{dc}(k)$  needs to be taken into account when the related reference signals are calculated. In fact, from the dc-Link voltage reference  $V^*_{dc}(k)$  and the reactive power reference  $Q^*_s(k)$  at the instant  $k$ , it is possible to calculate, knowing the ac current values, the active power reference at the time instant  $k+2$ ,  $P^*_s(k+2)$ . The required change in the active power flow to regulate the voltage at the desired value is given by (16), where  $N$  denotes the number of time steps required for reaching the target

$$P_{DC}(k+2) = \frac{c}{N_h} [V_{dc}^*(k+2) - V_{dc}^2(k+1)] \quad (13)$$

The load active power reference can be calculated as in (17), where  $i_{l1}(k) = [i_{l1}(k) \ i_{l2}(k)]^T$  represents the vector of the first harmonic of the load current

$$P_l^*(k+2) = \underline{v}_s^T(k) \begin{pmatrix} 2 & 1 \\ 1 & 2 \end{pmatrix} \underline{i}_{l2}(k) \quad (14)$$

Thanks to the high controller sampling frequency, it is acceptable to approximate  $i_{l1}(k) = i_{l1}(k+2)$ . The active power  $P^*_s(k+2)$  is simply obtained by filtering (17) with a digital resonant filter having a resonance frequency equal to 50 Hz. Finally, the total reference power at the supply side is therefore

$$P_s^*(k+2) = P_l^*(k+2) + P_{DC}(k+2) \quad (15)$$

Equation (15), together with  $Q^*_s(k+2) = 0$  (to ensure unity power factor operation of the system) and  $V^*_{dc}(k+2)$  constitute the reference set for the cost function.

### FUZZY LOGIC CONTROLLER

In FLC, basic control action is determined by a set of linguistic rules. These rules are determined by the system. Since the numerical variables are converted into linguistic variables, mathematical modeling of the system is not required in FC.

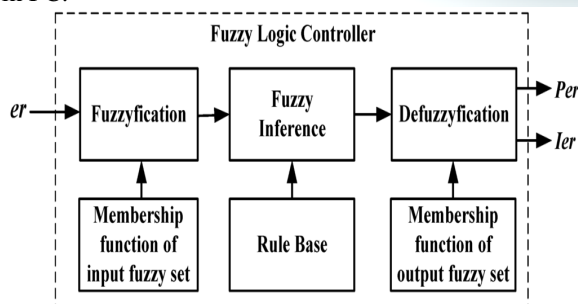


Fig.7.Fuzzy logic controller

The FLC comprises of three parts: fuzzification, inference engine and defuzzification. The FC is characterized as i. seven fuzzy sets for each input and output. ii. Triangular membership functions for simplicity. iii. Fuzzification using continuous universe of discourse. iv. Implication using Mamdani's, 'min' operator. v. Defuzzification using the height method.

TABLE : Fuzzy Rules

$e$	NB	NM	NS	ZE	PS	PM	PB
NB	NB	NB	NB	NB	NM	NS	ZE
NM	NB	NB	NB	NM	NS	ZE	PS
NS	NB	NB	NB	NS	ZE	PS	PM
ZE	NB	NM	NS	ZE	PS	PM	PB
PS	NM	NS	ZE	PS	PM	PB	PB
PM	NS	ZE	PS	PM	PB	PB	PB
PB	ZE	PS	PM	PB	PB	PB	PB

**Fuzzification:** Membership function values are assigned to the linguistic variables, using seven fuzzy subsets: NB (Negative Big), NM (Negative Medium), NS (Negative Small), ZE (Zero), PS (Positive Small), PM (Positive Medium), and PB (Positive Big). The Partition of fuzzy subsets and the shape of membership  $CE(k)$   $E(k)$  function adapt the shape up to appropriate system. The value of input error and change in error are normalized by an input scaling factor. In this system the input scaling factor has been designed such that input values are between -1 and +1. The triangular shape of the membership function of this arrangement presumes that for any particular  $E(k)$  input there is only one dominant fuzzy subset. The input error for the FLC is given as

$$E(k) = \frac{P_{ph}(k) - P_{ph}(k-1)}{V_{ph}(k) - V_{ph}(k-1)} \quad (16)$$

$$CE(k) = E(k) - E(k-1) \quad (17)$$

**Inference Method:** Several composition methods such as Max-Min and Max-Dot have been proposed in the literature. In this paper Min method is used. The output membership function of each rule is given by the minimum operator and maximum operator. Table 1 shows rule base of the FLC.

**Defuzzification:** As a plant usually requires a non-fuzzy value of control, a defuzzification stage is needed. To compute the output of the FLC, „height“ method is used and the FLC output modifies the control output. Further, the output of FLC controls the switch in the inverter. In UPQC, the active power, reactive power, terminal voltage of the line and capacitor voltage are required to be maintained. In order to control these parameters, they are sensed and compared with the reference values. To achieve this, the membership functions of FC are: error, change in error and output

The set of FC rules are derived from

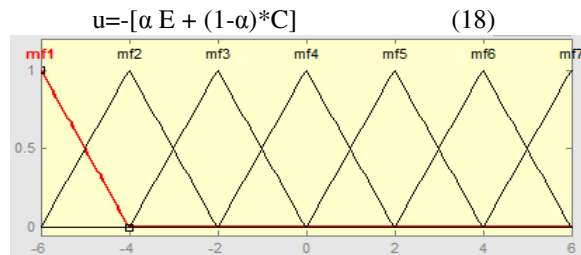


Fig 8 input error as membership functions

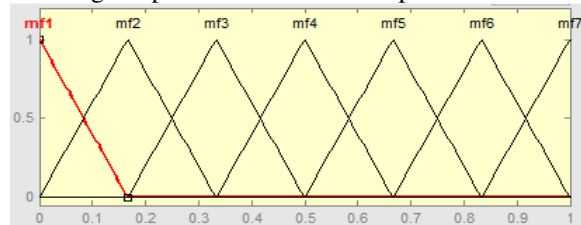


Fig 9 change as error membership functions

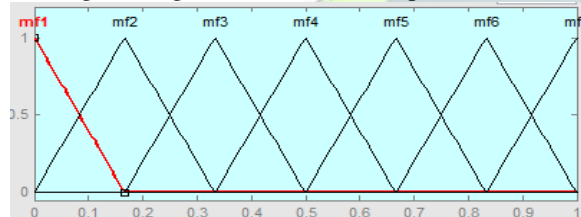
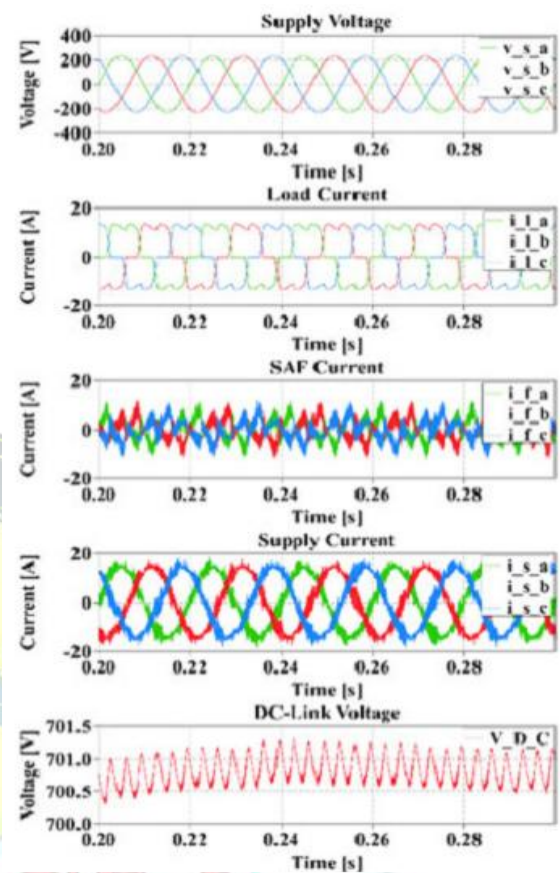


Fig.10 output variable Membership functions

Where  $\alpha$  is self-adjustable factor which can regulate the whole operation.

### SIMULATION RESULTS

Fig. 4 shows the M 2 PC effectiveness at rated conditions [see Fig. 4(b)] and the proposed control response to filter inductance variations around the nominal value.



(a)



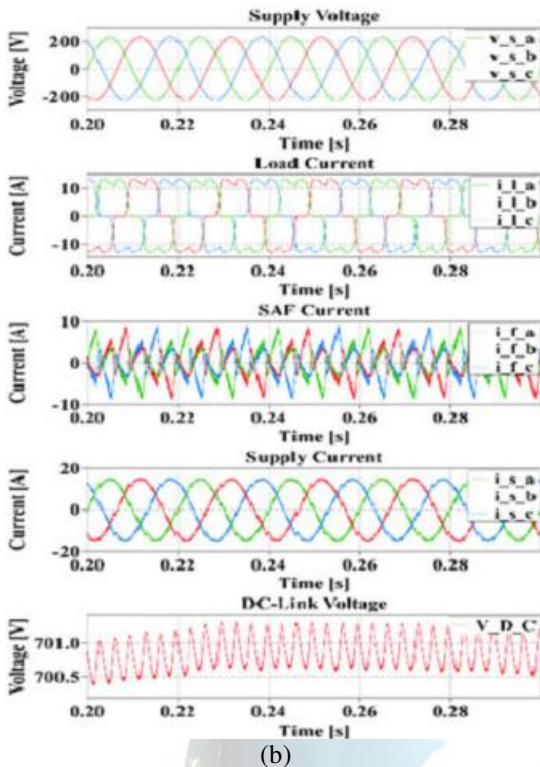


Fig. 4. M2PC sensitivity to filter inductance variation: (a)  $L_f = 2.375$  mH; (b)  $L_f = 4.75$  mH;

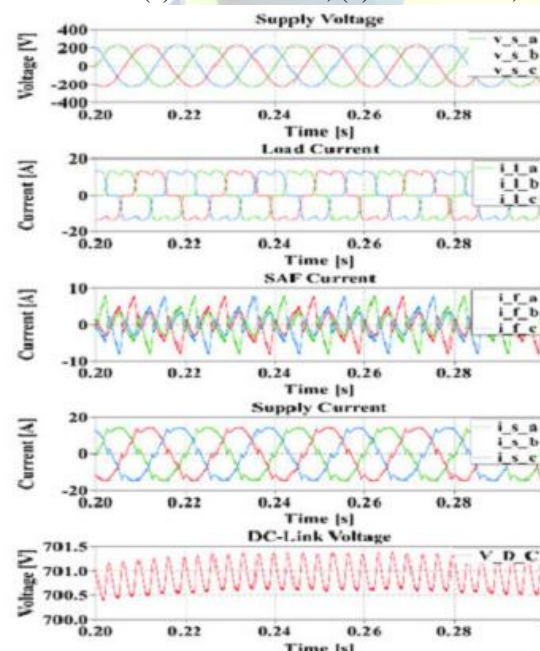


Fig. 4. M2PC sensitivity to filter inductance variation: (c)  $L_f = 9.5$  mH.

On the other hand, when the filter inductance varies the control performance starts degrading, but still maintains a stable and acceptable

behavior for large mismatch of  $L_f$  hence ensuring a good control robustness. In particular when the filter inductance value is lower than the nominal value higher frequency distortions, related with the degraded modulation performance, are present. Vice versa, when the filter inductance value is higher than the nominal value, lower frequency distortions, related with a control tracking delay, are present. In any case, the M2PC control is able to maintain stable operation with slightly downgraded performance for filter inductance variations from 50% to 200% the nominal value, as shown in Table I.

### CONCLUSION

In this paper we are implementing the SAF for harmonic distortion reduction regulated by an improved modulated model predictive controller. Based on the system model, it dynamically predicts the values of all the variables of interest in order to obtain a multiple control target optimization by minimizing a user defined cost function. Moreover the higher current ripple typical of MPC has been considerably reduced by introducing a cost function based modulation strategy without compromising the dynamic performances. Here we are included the fuzzy control for the better performance because it work like a human brain. By using simulation we can verify the SAF proposed system in both the transient conditions and steady state. It was hence demonstrated that FCS-M2PC is a viable and effective solution for control of active power compensators, where different systems variables can be regulated with the aid of only a single control loop, with no need for grid synchronization devices.

### REFERENCES

- [1] P. Salmeron and S. P. Litran, "Improvement of the electric power quality using series active and shunt passive filters," IEEE Trans. Power Del., vol. 25, no. 2, pp. 1058–1067, Apr. 2010.
- [2] H. Johal and D. Divan, "Design considerations for series-connected distributed FACTS converters," IEEE Trans. Ind. Appl., vol. 43, no. 6, pp. 1609–1618, Nov.-Dec. 2007.
- [3] D. Divan and H. Johal, "Distributed FACTS—A new concept for realizing grid power flow control," IEEE Trans. Power Electron., vol. 22, no. 6, pp. 2253–2260, Dec. 2007.
- [4] Christo Ananth, W. Stalin Jacob, P. Jenifer Darling Rosita. "A Brief Outline On ELECTRONIC DEVICES & CIRCUITS.", ACES Publishers, Tirunelveli, India, ISBN: 978-81-910-747-7-2, Volume 3, April 2016, pp:1-300.
- [5] M. L. Heldwein et al., "An integrated controllable network transformer—Hybrid active filter



system,"IEEE Trans. Ind. Appl., vol. 51, no. 2, pp. 1692–1701, Mar.-Apr. 2015.

[6] S. W. Mohod and M. V. Aware, "A STATCOM-Control scheme for grid connected wind energy system for power quality improvement,"IEEE Syst. J., vol. 4, no. 3, pp. 346–352, Sep. 2010.

[7] S. Wenchao and A. Q. Huang, "Fault-tolerant design and control strategy for cascaded h-bridge multilevel converter-based STATCOM,"IEEE Trans. Ind. Electron., vol. 57, no. 8, pp. 2700–2708, Aug. 2010.

[8] A. Hamadi, S. Rahmani, and K. Al-Haddad, "A hybrid passive filter configuration for VAR control and harmonic compensation,"IEEE Trans. Ind. Electron., vol. 57, no. 7, pp. 2419–2434, Jul. 2010.

[9] R. C. Dugan, M. F. McGranaghan, and H. W. Beaty, Electrical Power Systems Quality. New York, NY, USA: McGraw-Hill, 1996.

[10] H. Akagi, "The state-of-the-art of active filters for power conditioning," 2005 Eur. Conf. Power Electron. Appl., Dresden, Germany, pp. 1–15, 2005, doi: 10.1109/EPE.2005.219768. [11] S. Buso, L. Malesani, and P. Mattavelli, "Comparison of current control techniques for active filter applications," IEEE Trans. Ind. Electron., vol. 45, no. 5, pp. 722–729, Oct. 1998.

[12] P. Jintakosonwit, H. Fujita, and H. Akagi, "Control and performance of a fully-digital-controlled shunt active filter for installation on a power distribution system," IEEE Trans. Power Electron., vol. 17, no. 1, pp. 132–140, Jan. 2002.

IJARTET